Endoscopic Sentinel Node Biopsy is Less Invasive and Facilitated by SPECT-Fused 3D-CT Lymphography

By Koji Yamashita

Nippon Medical School, Japan

Abstract- Background: The endoscopic surgery for the breast diseases has been proven safe and aesthetic and named as video-assisted breast surgery (VABS). We also applied it for sentinel node (SN) biopsy. We firstly succeeded to fuse the single photon emission computed tomography (SPECT) with 3D-CT mammary lymphography (LG). It can show the detailed position of all SNs with or without RI uptake.

Method: In 3D-CT LG, 2 ml of Iopamidol 300 was injected subcutaneously above the tumor and the periareola. CT scan was taken 1 minute after injection to produce a 3D image of lymph ducts and nodes. In the lymphoscintigraphy, 99mTc phytate 74mBq was injected, and SPECT was taken after 2 hours. We fused it with 3D-CT LG. SN biopsy was performed endoscopically by dye and RI method.

Keywords: Radioisotope, Dye, Single photon emission computed tomography (SPECT), Endoscopic surgery, Sentinel lymph node biopsy, Lymphography, 3D-CT, Breast cancer.

GJMR-I Classification: NLMC Code: QZ 350

ENDOSCOPICSENTINELNODEBIOPSYISLESSINVASIVEANDFACILITATEDBYSPECT−FUSED3D−CTLYMPHOGRAPHY

Strictly as per the compliance and regulations of:

Endoscopic Sentinel Node Biopsy is Less Invasive and Facilitated by SPECT-Fused 3D-CT Lymphography

Koji Yamashita

Abstract- Background: The endoscopic surgery for the breast diseases has been proven safe and aesthetic and named as video-assisted breast surgery (VABS). We also applied it for sentinel node (SN) biopsy. We firstly succeeded to fuse the single photon emission computed tomography (SPECT) with 3D-CT mammary lymphography (LG). It can show the detailed position of all SNs with or without RI uptake.

Method: In 3D-CT LG, 2 ml of lopamidol 300 was injected subcutaneously above the tumor and the periareola. CT scan was taken 1 minute after injection to produce a 3D image of lymph ducts and nodes. In the lymphoscintigraphy, 99mTc phytate 74mBq was injected, and SPECT was taken after 2 hours. We fused it with 3D-CT LG. SN biopsy was performed endoscopically by dye and RI method. The endoscopic view showed stained lymph ducts and SNs, which can be navigated by RI detector gamma probe.

Results: We have performed SN biopsy with 3D-CT LG on 160 patients, RI with 3D-CT LG on 32 patients, and SPECT fused 3D-CT LG on 20 patients. We could detect the position of RI-positive SN on the axillary lymphatic mapping of SPECT-fused 3D-CT LG by a gamma probe during surgery. The average sampled number of SN was 2.3. The dye-negative SN and RI-negative SN could be removed endoscopically. There was no false negative study. The wound scars were only 1 cm long, and were inconspicuous and aesthetic.

Conclusions: The endoscopic SN biopsy is aesthetic and less invasive, which is facilitated by SPECT-fused 3D-CT LG.

Keywords: Radioisotope, Dye, Single photon emission computed tomography (SPECT), Endoscopic surgery, Sentinel lymph node biopsy, Lymphography, 3D-CT, Breast cancer.

I. Introduction

In early breast cancer, the presence of metastasis in axillary lymph nodes (AN) is an important factor in prognosis and further treatment. Sentinel node (SN) biopsy provides us valuable information about no need to dissect AN for node-negative patients [1, 2]. SN is defined as the first lymph node drained of lymph flow from the tumor [3, 4]. The most commonly used methods to identify the SN are dye-staining [5, 6] and radioisotope (RI) incorporation [7, 8]. We have reported the usefulness of multidetector-row three-dimensional computed tomography (3D-CT) mammary lympho-

Author: Department of Breast Surgery, Nippon Medical School, 1-5, Sendagi-1, Bunkyo-ku, Tokyo, Japan 113-8603.
e-mails: yamasita@nms.ac.jp, here@here.com

graphy (LG) for SN biopsy [9, 10, 11]. It can show the detailed relations between lymph ducts and lymph nodes in the axilla on the anatomical architecture [12]. And the late phase of 3D-CT LG of the breast can show the axillary lymphatic architecture from SN into venous angle [13].

3D-CT LG can decrease the false negative study of SN biopsy with RI and/or dye-staining methods. However, during surgery, we sometimes miss the exact node detected by 3D-CT LG, because the discrepancy of SN exists between RI, dye, and 3D-CT LG. Up to the present, we have used the skin marking with oil pen projected by the laser pointer of CT. The single stained node can be found easily, but multiple adjacent nodes cannot be distinguished each other.

The conventional lymphoscintigraphy shows the RI-uptaken nodes, but it cannot show its exact location. Single photon emission computed tomography (SPECT) show the exact location of RI-uptaken nodes in the anatomical architecture. We firstly succeeded to fuse this SPECT with our 3D-CT LG. It can show the RI-uptaken nodes are coincided with some of the enhanced SNs by 3D-CT LG. Some SNs of 3D-CT LG included RI-uptaken nodes, and dye-stained nodes, and bi-negative nodes. We can notice the location of RI-uptaken nodes in the SN mapping of 3D-CT LG. During surgery, RI detector probe can navigate hot node. We can find the other nodes relative to these hot nodes in SN mapping of 3D-CT LG.

II. Materials and Methods

a) Patients

From July 2002 to March 2010, 700 patients with breast disease were treated surgically by us in the Department of Surgery at the Nippon Medical School of Musashikosugi Hospital and Main Hospital. We performed video-assisted breast surgery (VABS) for the patients with a limited small breast cancer at surgery [14, 15]. We also performed SN biopsy for the patients without clinical axillary node metastasis. A SN biopsy was performed for 200 patients, 160 of which involved SN biopsy using VABS and 3D-CT LG. The patient characteristics are shown in Table 1. Down-staged cases treated by preoperative systemic chemotherapy (PST) are included. For example, the patient with large

1

tumor of 10 cm in diameter gained pathological complete remission (pCR) after PST. These patients did not have any clinical metastasis of axillary nodes after PST.

b) 3D-CT lymphography

Interstitial 3D-CT LG was performed using a 16-channel multidetector-row helical 3D-CT scanner (Toshiba Aquilion 16; Toshiba Medical Systems Corporation, Tochigi, Japan). The patients were placed in the supine position with arms positioned in the lateral abduction direction suitable for the operating position. After local anesthesia by subcutaneous injection of 1% lidocaine (0.5 ml), 2 ml of contrast enhancing material iopamidol (Iopamiron 300; Nihon Shering, Osaka, Japan) were injected intracutaneously into the periareolar skin and the skin above the tumor. A CT image with a 3-mm slice thickness was taken 1 and 5 minutes after injection. SN was identified on transaxial CT images, and their location was marked on the skin surface with an oil-painting pen using a laser pointer of CT the day before the surgery. Next, 3D-CT images were reconstructed from transaxial enhanced CT images, which clearly showed the lymph ducts and SN. 3D-CT LG was also performed for the arm LG. 2 ml of iopamidol were injected in the upper inner arm along the medial intramuscular groove of the ipsilateral arm after local anesthesia. A CT image was taken 5 minutes after injection on the same condition.

c) Spect

On the day before surgery, 74 MBq technetium 99m (99mTc) phytate (FUJIFILM RI Pharma Co., LTD., Tokyo, Japan) in sterile saline (total volume 1 mL) was injected intradermally into two different sites of the skin above the tumor and around the periareola. Lymphoscintigraphy and SPECT were performed 2 hours after injection of radio colloid. If one or more focal accumulations of radioactivity (hot spots) were visualized, these were assumed to be SNs. Small amount of RI markers were positioned on the jagular notch of sternum and the xiphoid process to correct the fusion points. We used the image fusion software Syntegra [16] (Philips Medical Systems, Eindhoven, The Netherlands) and Real INTAGE (KGT, Tokyo, Japan) to fuse SPECT data with 3D-CT LG.

d) Surgical methods

Previously, VABS has been described in detail [15]. The following operative procedures were performed: skin incision in the axilla and/or periareola, skin flap formation via the tunnel method [17], pectoral muscle fascia dissection, vertical section of the mammary gland, SN biopsy by the dye-staining method guided by preoperative 3D-CT LG marking, and axillary node dissection (levels 1 and 2). Radiotherapy and chemotherapy were performed for malignant diseases.

The SN biopsy was performed by the dye-staining method using a part of the VABS technique at the beginning of the operation before gland resection. In the periareolar region and over the tumor, 2 ml of 1% indocyanine green were injected subcutaneously. A 1-cm-long skin incision was made along wrinkles in the axilla at the position marked by 3D-CT LG. A Visiport optical trocar (Covidien Japan, Tokyo, Japan) was inserted into the incision after 20 minutes. The endoscopic view was observed through the Visiport with a 10-mm-diameter straight-angled rigid endoscope (Olympus Optical, Tokyo, Japan), and the stained nodes were found by following the dye in the lymph ducts. RI detector probe NAVIGAOR GPS system (Covidien Japan, Tokyo, Japan) was used for detecting RI-uptaken nodes.

The lymph nodes were sampled, and metastasis was determined from fast frozen sections. To remove them, we left the external tube of the Visiport and grasped the nodes by the endodissector (Johnson & Johnson Company, New Brunswick, NJ, USA), then cut and shielded the surrounding lymph duct and vessels using the harmonic scalpel (Johnson & Johnson Company). Axillary node dissection was performed at levels 1 and 2 with bipolar scissors through the same incision, which was lengthened to 2.5 cm. The inferior pectoral nerve, long thoracic nerve, second and third intercostobrachial nerves, thoracodorsal nerve, artery, and vein were observed and preserved. The lateral pectoral artery was preserved for the lateral tissue flap. After surgery, SN and axillary nodes were pathologically examined by standard hematoxylin and eosin staining. Breast reconstruction was simultaneously performed either by mobilization of the remnant mammary gland and by filling the lateral thoracic fat tissue flap (LTF) or by filling an absorbent synthetic fiber [17].

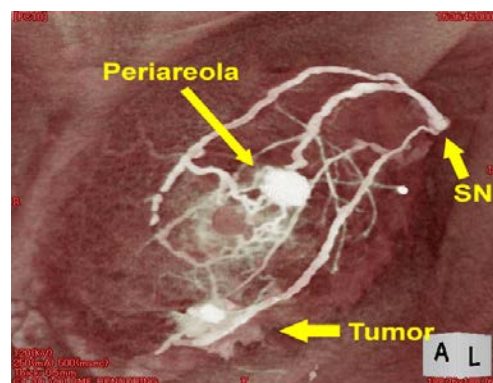Informed consent for the procedure was obtained from all the patients before surgery.

Fig.1 : 3D-CT lymphography (LG) showed the lymphatic system from the breast to the sentinel node (SN). The periareolar lymphatic flow was draining from the tumor or from the other area of the breast. It was circling around the nipple-areolar complex and going into SN in the axilla. Some lymph ducts from the tumor were going directly into SN
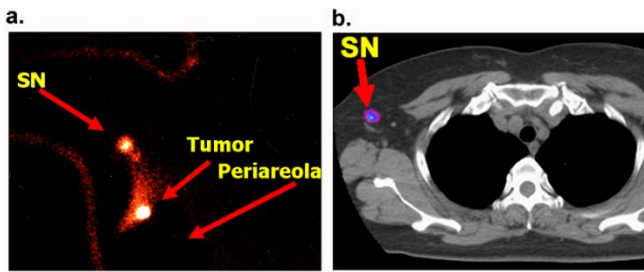
Fig.2 :   *a.*   Lymphoscintigraphy
The conventional lymphoscintigraphy shows only information about the existence of nodes with an uptake of RI as hot spots

b.   Single photon emission computed tomography (SPECT)
SPECT-CT can show the exact location of the hot spots on the axial view of the CT image, as showing in the figure. They are always coincided with the axillary nodes.
SN: sentinel node

III. Results

We have performed 3D-CT LG on 160 patients, and the lymphoscintigraphy with 3D-CT LG on 32 patients. 3D-CT LG clearly showed the precise lymphatic flow from the tumor to SN (Fig 1). It showed periareolar circular lymph ducts and complicated radial breast subcutaneous lymph ducts flow. They were connected to make a network. It can show SN at only one minute after injection. By following up to 5 minutes, we can follow the lymph ducts beyond SN into the second to the fifth node groups toward the venous angle with complex plexus, observed in the surrounding anatomical architecture. The conventional lymphoscintigraphy shows only information about the existence of nodes with the uptake of RI as hot spots (Fig 2a). We injected isotope 99m technetium phytate 74MBq into the subcutane over the tumor and the periareola on the day before surgery. The hot spots were observed, however, they cannot show the exact location of them on the anatomical structure and the relations between lymph ducts and lymph nodes.

SPECT-CT can show the exact location of the hot spots on the axial view of the CT image, as showing in the figure (Fig 1b). They are always coincided with the axillary nodes. However, it cannot show the lymph ducts and the relations between lymph ducts and nodes either. The number of hot spots was usually only one or two. The average number was 1.2, which was less than the number 2.3 of SN found by 3D-CT LG.

We fused the DICOM data of SPECT with 3D-CT LG by using the image fusion software (Fig 3). The hot spot can be coincided with enhanced SN observed on 3D-CT LG. However, not all of SNs had a hot spot. We call SN with a hot spot as a hot node and SN without a hot spot as a cold node. We can recognize the location of the cold nodes by using the relation to the hot nodes on the map of 3D-CT LG.

We experienced a profitable case to show this benefit (Fig 4a). The 3D-CT LG shows the lymph duct divides into three branches and into three sentinel nodes. We call the blue stained node as a blue node and the unstained node as a gray node in the dye staining method. SPECT-fused 3D-CT LG shows that the first one is hot and blue, the second one is cold and blue, and the third one is cold and gray (Fig 3b). The metastasis was found in the second one. We can detect the forth nodes, cold and gray. It was also metastasized. However, the other axillary lymph nodes were not metastasized.

SN can be classified into four types under RI uptake and dye stainability. We summarized the number of the cases with these four types of SNs in Table 2. We have examined 3D-CT LG with RI on 32 patients and with SPECT on 20 patients. 25% of these patients had cold nodes. The metastasis was found on 6 patients. And on 2 patients the cold and blue nodes had metastases.
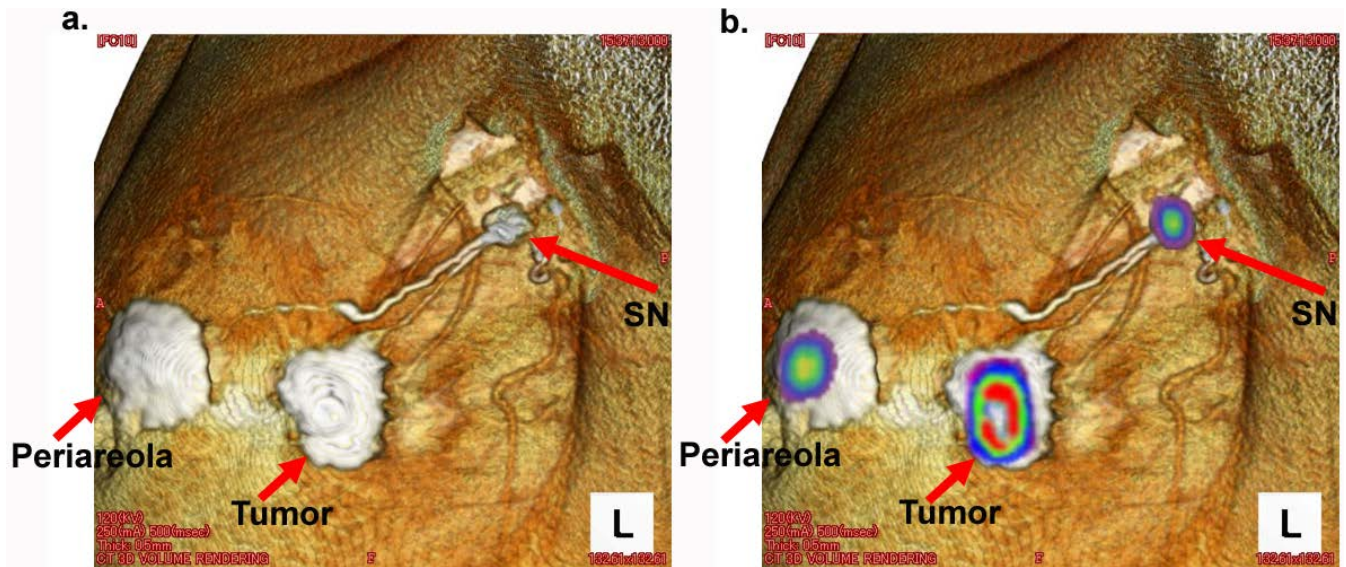
Fig.3 : a. 3D-CT lymphography (LG)

The contrast enhancing materials flow from the injected sites over the tumor and the periareola through the two lymph ducts into single SN in the axilla.

b. SPECT-fused 3D-CT LG

DICOM data of SPECT was projected on 3D-CT LG. The hot spots were coincided with SN detected by 3D-CT LG.

Fig.4 : a. 3D-CT lymphography (LG)

The lymph duct from the tumor were divided to three branches and into three SN shown as enhanced nodes (#1, #2, and #3) in 3D-CT LG. Node #4 is thought to be flown from the node #2.

b. SPECT-fused 3D-CT LG

The hot spot was observed only on the node #1. The blue stained nodes were the node #1 and #2. The other nodes were cold and gray. The node metastasis was found in the node #2 and #4.a. 3D-CT lymphography (LG)

The contrast enhancing materials flow from the injected sites over the tumor and the periareola

Table 1 : Patient Characteristics

	3D-CT LG		RI + 3D-CT LG	
	Mean	Range	Mean	Range
Age (y/o)	54.9	26 - 82	57.4	26 - 82
Tumor size (cm)	1.9	0.1 – 10	1.4	0.1 – 1.3
	Number	%	Number	%
Tis	4	1.9	4	12.5
T1a / T1b / T1c	3 / 20 / 86	1.9 / 12.5 / 53.8	1 / 2 / 18	3.1 / 6.2 / 56.3
T2	51	31.9	7	21.9
Lymph node metastasis (N)	40	25.0	6	18.8
Distant metastasis (M)	0	0	0	0
ER (+/-)	105 / 55	65.6	26 / 6	81.2
PgR (+/-)	84 / 76	52.5	19 / 13	59.4
HER2 (+/-)	38 / 122	23.7	3 / 29	9.4
Total	160		32	

3D-CT LG: 3-dimensional computed tomography of lymphography, RI: radioisotope

ER: estrogen receptor, PgR: progesterone receptor, HER2: human epidermal growth factor receptor type 2

Table 2 : RI uptake, dye-stainability, and node metastasis

	RI	Dye	Meta
#1	+	+	−
#2	−	+	+
#3	−	−	−
#4	−	−	+

RI: radioisotope, Meta: node metastasis

Table 3 : The number of each type of SN

Nodes	N	RI	+	−	
		Dye	+	−	+	−
3D-CT LG	32		26	3	6	2
SPECT 3D-CT LG	20		16	2	4	1

The four types of SN are classified as to RI uptaken or not, and as dye stained or not.

IV. DISCUSSIONS

We previously reported that 3D-CT LG could show the precious lymphatic architecture of the breast and the axilla, and its usefulness in SN biopsy [13, 14, 18]. It is not sure that there is only one node defined as SN. And the lymph duct from the breast and the tumor to SN is not always single. However, the lymphoscintigraphy shows an only single hot node without showing the other SNs. The other nodes adjacent to the hot node can be sampled when they are stained with blue dye. On the other hand, SN distant from the hot node cannot be sampled. 3D-CT LG shows the detailed relations of SNs and lymph ducts from the breast. It enables us to sample this distant SN. The gray nodes adjacent to SN can also be recognized as SN or not, by 3D-CT LG.

During surgery, we have to project the mapping of 3D-CT LG on the patient body. We usually mark the position of SN on the skin by oil pen at the laser pointer of CT. It is not sharp positioning because of the distance from the skin to SN in the deep axilla. The anchoring needle is often used for the non-palpable mass with calcifications in the mammary gland. It may be useful for SN marking, but it has a danger to harm surrounding vessels in the axilla. The dye injection on the SN may be useful, but it is diluted and absorbed in the tissue. It confuses the stained ducts and nodes, because we don't have enough colors of dye to be distinguished between them. The ultrasonography may find the swelling nodes. It was reported to be synchronized to the CT-LG data. It can show the location of SN, but it is disturbed by air and it cannot navigate us to find SN during surgery. Therefore, the dye injection is needed with a guidance of ultrasound. RI detector gamma probe can show the location of a hot node and navigate us to find a hot SN easily during surgery. Its location is projected on the SN mapping of 3D-CT LG. We can sample not only these hot nodes but also the other cold SN with relative node positions indicated by SPECT-fused 3D-CT LG. The dye staining method also helps us to find the hot SNs and the cold SNs.

We have performed endoscopic surgery for breast diseases, named as video-assisted breast surgery (VABS) [19, 20]. And we have reported about the advantage of the endoscopic SN biopsy [21]. It can remove SN by a direct approach from the skin without detachment of the surrounding tissues. Therefore it becomes to be less invasive than the conventional open biopsy. It needs only 1 cm long skin incision and leaves an inconspicuous scar in the axilla. We can observe the dye stained ducts and nodes on the endoscopic view through the optical trocar Visiport. We proceed into the fat tissue of the axilla bluntly and cut thin fascia sharply by the small knife of Visiport. Even when it is difficult to find the dye because of the narrow field of vision, we can find the hot nodes easily by the RI detector gamma probe. SPECT-fused 3D-CT LG helps us to anchor these hot SN in order to navigate detecting all the other nodes on the mapping. We succeeded in the endoscopic SN biopsy on all cases.

In Figure 4, the lymph duct from the tumor branched to three and into three different SNs. Only node #2 was a cold-blue node and had metastasis. We might get into a danger of false negative study when SN biopsy was performed only with RI method. SPECT-fused 3D-CT LG presents the locational relations between hot nodes and cold nodes. SN biopsy with 3D-CT LG presents the relations between dye-stained blue nodes and unstained gray nodes. The numbers of the patients with these nodes are listed in Table 2. 25% of the patients had the cold nodes. Two patients with cold-blue nodes had metastasis in their nodes. One patient with cold-gray nodes had metastasis. They may be a cause of false negative study, but they could evade such a danger by SPECT-fused 3D-CT LG.

The fluorescence study can show the precise lymph flow in mice, but in a human study the thick subcutaneous fat tissue disturbs the permeability of fluorescence to be visualized through the skin [22, 23]. A new approach of lymphangiography has been reported by using MRI in mice [24, 25]. It can show the precise lymphatic system in the anatomical architecture. It will be helpful for us to perform the selective axillary dissection and to preserve the arm lymph channel, like 3D-CT LG. However, it needs long time to exam, so it cannot follow the rapid lymph flow as one minute after injection like CT.

V. CONCLUSION

The endoscopic SN biopsy is aesthetic and less invasive, and SPECT-fused 3D-CT LG is valuable to improve the precision of SN biopsy and to facilitate it by RI navigation.

VI. Acknowledgements

References Références Referencias

1. Veronesi U, Paganelli G, Galimberti V. Sentinel-node biopsy to avoid axillary dissection in breast cancer with clinically negative lymph nodes. Lancet 1997; 349:1864-7.
2. Schrenk P, Rieger R, Shamiyeh A. Morbidity following sentinel lymph node biopsy versus axillary lymph node dissection for patients with breast carcinoma. Cancer 2000; 88:608-14.
3. Schwartz GF, Giuliano AE, Veronesi U. Proceedings of the consensus conference on the role of sentinel lymph node biopsy in carcinoma of the breast April 19 to 22, 2001, Philadelphia, Pennsylvania. Cancer 2002; 94:2542-51.
4. Kuehn T, Bembenek A, Decker T. A Concept for the Clinical Implementation of Sentinel Lymph Node Biopsy in Patients with Breast Carcinoma with Special Regard to Quality Assurance. Cancer 2005; 103:451-461.
5. Giuliano AE, Kirgan DM, Guether V. Lymphatic mapping and sentinel lymphadenectomy for breast cancer. Ann Surg 1994; 220:391-8.
6. Borgstein PJ, Meijer S, Pijpers R. Intradermal blue dye to identify sentinel lymph-node in breast cancer. Lancet 1997; 384:149-57.
7. Krag DN, Weaver DL, Alex JC. Surgical resection and radiolocalization of the sentinel lymph node in breast cancer using a gamma probe. Surg Oncol 1993; 2(6):335-9.
8. Mariani G, Moresco L, Viale G. Radioguided sentinel lymph node biopsy in breast cancer surgery. J Nucl Med 2001; 42:1198-1215.
9. Suga K, Ogasawara N, Okada M. Interstitial CT lymphography-guided localization of breast sentinel lymph node: preliminary results. Surgery 2003; 133:170-179.
10. Tangoku A, Yamamoto S, Suga K. Sentinel lymph node biopsy using computed tomography-lymphography in patients with breast cancer. Surgery 2004; 135:258-265.
11. Minato M, Hirose C, Sasa M. 3-Dimensional computed tomography lymphography-guided identification of sentinel lymph node in breast cancer patients using subcutaneous injection of nonionic contrast medium. A clinical trial. J Comput Assist Tomogr 2004; 28:46-51.
12. Yamashita K, Shimizu K. Video-assisted Breast Surgery and Sentinel Lymph Node Biopsy guided by 3D-CT lymphography. Surg Endosc 2008; 22: 392-297, DOI: 10.1007/s00464-007-9407-5.
13. Yamashita K, Shimizu K. Evaluation of sentinel lymph node metastasis alone guided by three-dimensional computed tomographic lymphography in video-assisted breast surgery. Surg Endosc 2009; 23:633–640, DOI 10.1007/s00464-008-9809-z.
14. Yamashita K, Shimizu K. Endoscopic Video-Assisted Breast Surgery: Procedures and Short-Term Results. J Nippon Med Sch 2006; 73:193-202.
15. Yamashita K, Shimizu K. Video-Assisted Breast Surgery: Reconstruction More than 33% Resected Breast. J Nippon Med Sch 2006; 73:320-327.
16. Sykes JR, Amer A, Czajka J, Moore CJ. A feasibility study for image guided radiotherapy using low dose, high speed, cone beam X-ray volumetric imaging. Radiother Oncol 2005; 77:45-52.
17. Yamagata M, Takasugi T, Takayama T. Partial mastectomy by the periareolar incision. Geka Chiryo 2002; 86:932-940.
18. Yamashita K, Shimizu K, 3D-CT Lymphography for Mapping Metastatic Breast Sentinel Node and Axillary Nodes. In: Leong S (eds) From Local Invasion to Metastatic Cancer: Involvement of Distant Sites through the Lymphovascular System. Humana Press, Springer, Totowa, 2009: Chapter 14: 159-168.
19. Yamashita K, Shimizu K. Transaxillary retromammary route approach of video-assisted breast surgery enables the inner side breast cancer to be resected for breast-conserving surgery. Am J Surg 2008; 196:578–581
20. Yamashita K, Shimizu K.. Trans-axillary retro-mammary gland route approach of video-assisted breast surgery can perform breast conserving surgery for cancers even in inner side of the breast. Chin Med J 2008; 121: 1960-1964.
21. Yamashita K, Shimizu K. Video-assisted breast surgery can sample the second and third sentinel nodes to omit axillary node dissection for sentinel-node positive patients. Surg Endosc 2009; 23, 1574-1580, DOI 10.1007/s00464-009-0343-4.
22. Hojo T, Nagao T, Kikuyama M, Akashi S, Kinoshita T. Evaluation of sentinel node biopsy by combined fluorescent and dye method and lymph flow for breast cancer. Breast. 2010; DOI 10.1016/ j. breast. 2010.01.014.
23. Murawa D, Hirche C, Dresel S, Hünerbein M. Sentinel lymph node biopsy in breast cancer guided by indocyanine green fluorescence. Br J Surg 2009; 96(11):1289-94.
24. Kobayashi H, Kawamoto S, Choyke PL, et al. Comparison of Dendrimer-Based Macromolecular Contrast Agents for Dynamic Micro-Magnetic Resonance Lymphangiography. Magn Reson Med 2003; 50:758–766.

25. Koyama Y, Talanov VS, Bernardo M, et al. A Dendrimer-Based Nanosized Contrast Agent Dual-Labeled for Magnetic Resonance and Optical Fluorescence Imaging to Localize the Sentinel Lymph Node in Mice. J Magn Reson Imaging 2007; 25:866–871.

This page is intentionally left blank